

# **Spatial variability of $^{10}\text{Be}$ in deep ice and the influence of the measurement procedure - supplementary information**

**Niklas Kappelt<sup>1</sup>, Piers Larkman<sup>2</sup>, Pascal Bohleber<sup>2,3</sup>, Florian Adolphi<sup>2</sup>, Marcus Christl<sup>4</sup>, Christof Vockenhuber<sup>4</sup>, Philip Gautschi<sup>4</sup>, Eric Wolff<sup>5</sup>, and Raimund Muscheler<sup>1</sup>**

<sup>1</sup>Department of Geology, Lund University, Sölvegatan 12, 22362 Lund, Sweden

<sup>2</sup>Department of Geosciences, Alfred Wegener Institute Helmholtz Centre for Polar and Marine Research, Am Handelshafen 5, 27570 Bremerhaven, Germany

<sup>3</sup>Goethe University Frankfurt am Main, Altenhöferallee 1, 60438 Frankfurt am Main, Germany

<sup>4</sup>Laboratory of Ion Beam Physics, Swiss Federal Institute of Technology, Otto-Stern Weg 5, 8093 Zürich, Switzerland

<sup>5</sup>Department of Earth Sciences, University of Cambridge, Downing Street, CB2 3EQ Cambridge, United Kingdom

**Correspondence:** Niklas Kappelt (niklas.kappelt@geol.lu.se)

Figure S1 shows the cutting plan for A-cut pieces from EDC and indicates the surface which was scanned with the xLASM system.

### Sampling and cutting plan

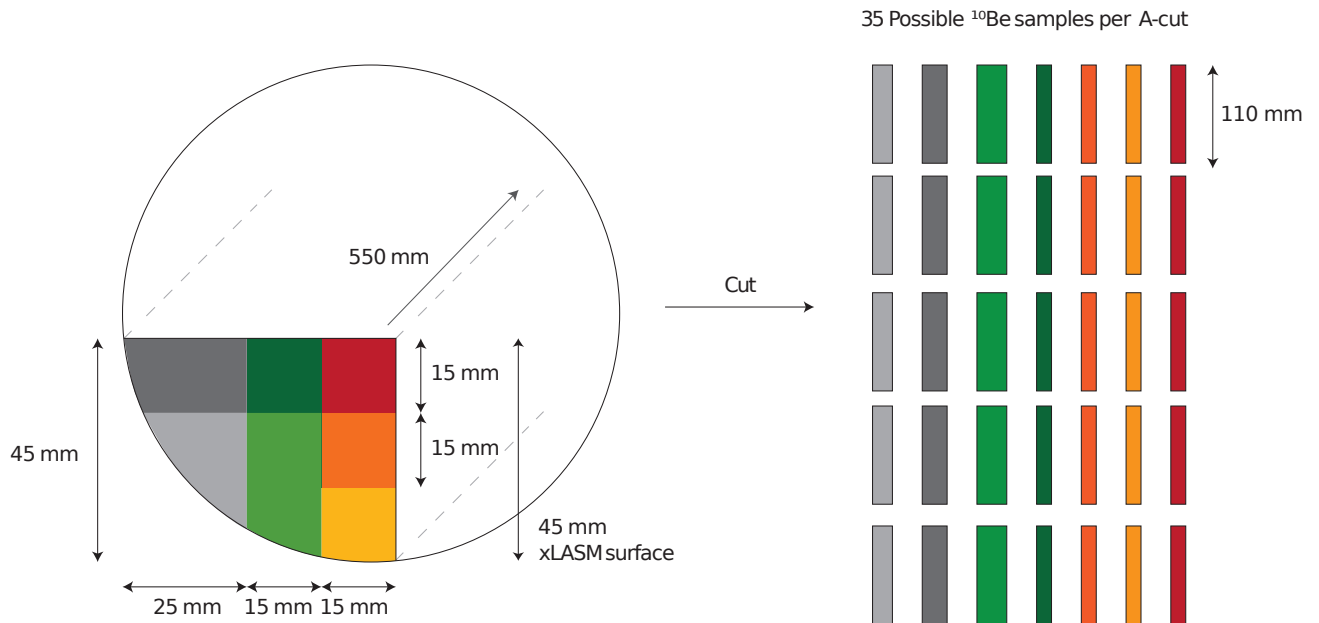


**Figure S1.** Cutting plan.

Table S1 lists the EDC samples and their respective depths and ages.

**Table S1.** EDC sample selection.

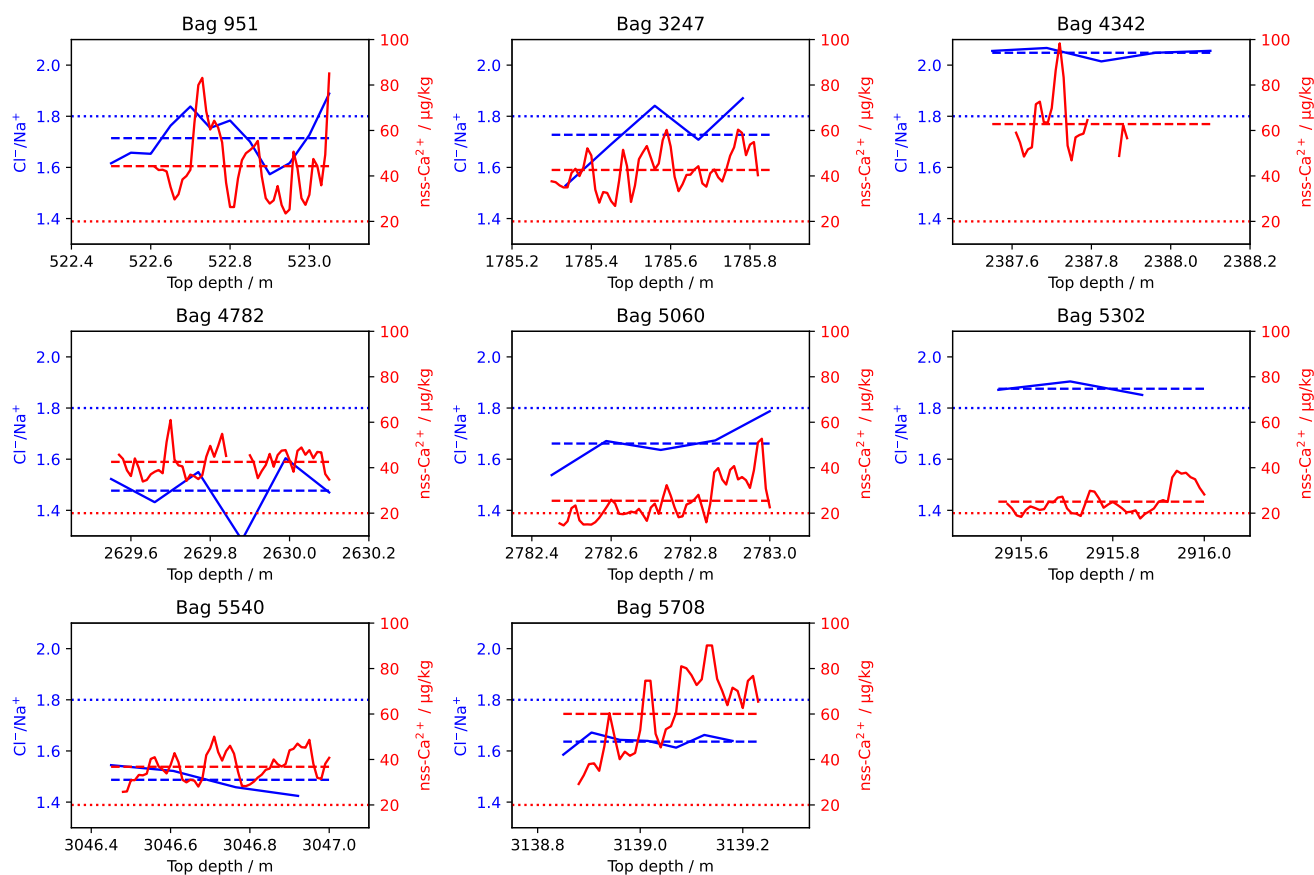
Bag	Depth <sub>top</sub>	Depth <sub>bot</sub>	Age / yr BP
951	522.50	523.05	21,954
3247	1785.30	1785.85	138,770
4342	2387.55	2388.10	272,503
4782	2629.55	2630.10	358,368
5060	2782.45	2783.00	429,744
5302	2915.55	2916.00	544,440
5540	3046.45	3047.00	646,708
5708	3138.85	3139.23	738,413

Table S2 lists the Skytrain samples and their respective depths and ages.

**Table S2.** Skytrain samples.

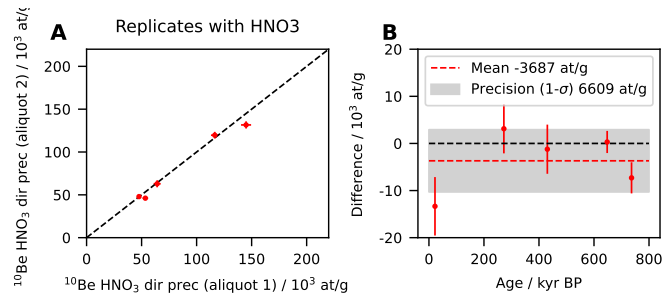
Depth <sub>top</sub>	Depth <sub>bot</sub>	Weight / g	Weight <sub>small</sub> / g	$^{10}\text{Be}$ / $10^4$ at/g	$^{10}\text{Be}_{\text{small}}$ / $10^4$ at/g
124.0	125.6	1243.4	81.0	$1.658 \pm 0.025$	$1.105 \pm 0.249$
485.6	487.2	1179.9	73.7	$3.075 \pm 0.047$	$3.566 \pm 0.205$
526.42	528.0	1208.4	72.6	$2.846 \pm 0.043$	$2.685 \pm 0.123$
552.8	554.4	1191.5	61.1	$2.468 \pm 0.038$	-
570.4	572.03	1243.8	70.1	$1.911 \pm 0.029$	$2.746 \pm 0.653$
597.6	599.2	1305.2	73.9	$2.809 \pm 0.043$	-
619.2	620.76	1203.8	73.7	$1.504 \pm 0.030$	$1.985 \pm 0.226$
636.0	637.64	1296.1	47.4	$2.090 \pm 0.035$	$3.150 \pm 0.483$
640.0	641.57	1072.2	40.9	$2.388 \pm 0.107$	-
644.8	646.42	1274.1	55.4	$1.548 \pm 0.024$	$1.563 \pm 0.210$

Figure S2 shows high-resolution  $\text{Cl}^-/\text{Na}^+$  ratio and  $\text{nss-Ca}^{2+}$  data from Lambert et al. (2012) and Wolff et al. (2010).



**Figure S2.**  $\text{Cl}^-/\text{Na}^+$  ratio and  $\text{nss-Ca}^{2+}$  data in bags of the requested radionuclide samples (Lambert et al., 2012; Wolff et al., 2010).

To determine the precision of repeat measurements with  $\text{HNO}_3$  treatment, the  $^{10}\text{Be}$  concentration was measured in two aliquots of homogenised sub-samples from different depths, which both received 2 mL 65 %  $\text{HNO}_3$  and were directly precipitated. Figure S3 shows the reproducibility between aliquots and the precision of  $6609 \text{ at g}^{-1}$ , taken as the one- $\sigma$  standard deviation of the differences shown in panel B. This is significantly larger than the standard deviation among blank samples prepared with  $\text{HNO}_3$  treatment and direct precipitation ( $560 \text{ at g}^{-1}$  in a 25 g sample).



**Figure S3.** **A**  $^{10}\text{Be}$  concentrations after treatment with 2 mL 65 %  $\text{HNO}_3$  and direct precipitation of Be in two aliquots of samples from different depths at EDC. The identity line, where  $y = x$ , is shown as a dashed line. **B** The differences between the two aliquots and their one- $\sigma$  standard deviation from the mean.

Figures S4 and S5 show the measured LASM images and the grain segmentation at two different depths. LASM measurements were also performed on samples from bags 4342, 4782, 5302, and 5708 suggest similar results, but the segmentation failed due to bad image quality.

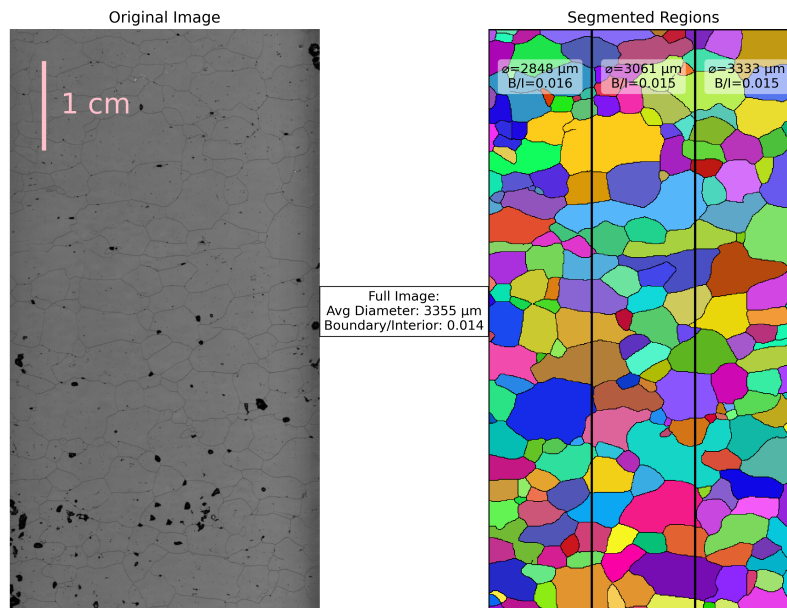


**Figure S4.** Original LASM image and grain segmentation from the EDC 3247 sample (age 139 kyr). The scale bar corresponds to both images.

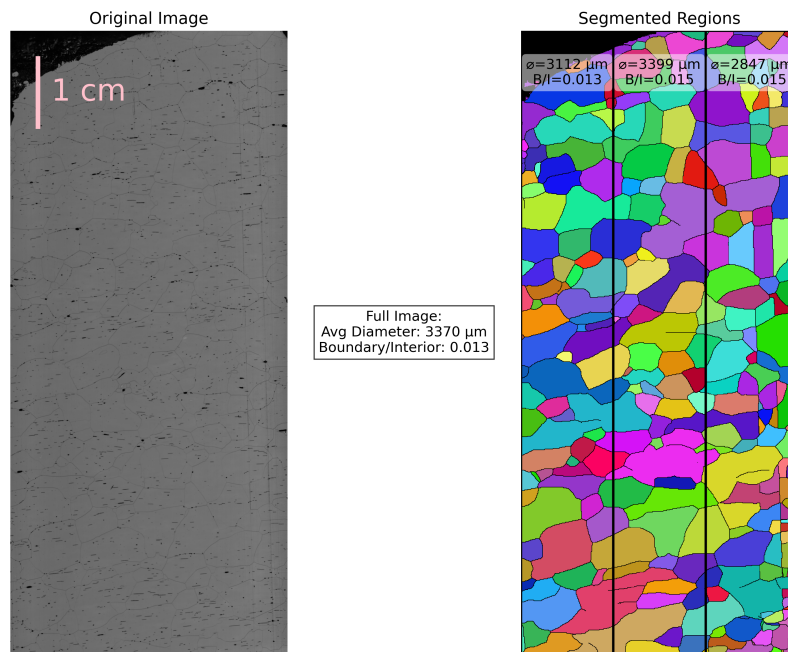


**Figure S5.** Original LASM image and grain segmentation from the EDC 5060 sample (age 430 kyr). The scale bar corresponds to both images.

## References

- Lambert, F., Bigler, M., Steffensen, J. P., Hutterli, M., and Fischer, H.: Centennial mineral dust variability in high-resolution ice core data from Dome C, Antarctica, *Climate of the Past*, 8, 609–623, <https://doi.org/10.5194/cp-8-609-2012>, 2012.
- Wolff, E. W., Barbante, C., Becagli, S., Bigler, M., Boutron, C. F., Castellano, E., de Angelis, M., Federer, U., Fischer, H., Fundel, F., Hansson, M., Hutterli, M., Jonsell, U., Karlin, T., Kaufmann, P., Lambert, F., Littot, G. C., Mulvaney, R., Röthlisberger, R., Ruth, U., Severi, M., Siggaard-Andersen, M. L., Sime, L. C., Steffensen, J. P., Stocker, T. F., Traversi, R., Twarloh, B., Udisti, R., Wagenbach, D., and Wegner, A.: Changes in environment over the last 800,000 years from chemical analysis of the EPICA Dome C ice core, *Quaternary Science Reviews*, 29, 285–295, <https://doi.org/10.1016/j.quascirev.2009.06.013>, 2010.